Received: 17 November 2019 | Revised: 1 July 2020 | Accepted: 8 July 2020

DOI: 10.1002/aic.16984

THERMODYNAMICS AND MOLECULAR-SCALE PHENOMENA

AIChE JOURNAL

Partitioning of water-soluble vitamins in biodegradable aqueous two-phase systems: Electrolyte perturbed-chain statistical associating fluid theory predictions and experimental validation

Kamila Wysoczanska[1] | Hoang Tam Do[2] | Gabriele Sadowski[2] | Eugénia A. Macedo[1] | Christoph Held[2]

[1]Associate Laboratory of Separation and Reaction Engineering—Laboratory of Catalysis and Materials (LSRE-LCM), Faculty of Engineering, University of Porto, Porto, Portugal

[2]Laboratory of Thermodynamics, Department of Biochemical and Chemical Engineering, Technische Universität Dortmund, Dortmund, Germany

Correspondence
Christoph Held, Laboratory of Thermodynamics, Department of Biochemical and Chemical Engineering, Technische Universität Dortmund, Emil-Figge-Street 70, 44227 Dortmund, Germany.
Email: christoph.held@tu-dortmund.de

Funding information
Acção Integrada, Grant/Award Number: A08/17; Deutsche Forschungsgemeinschaft, Grant/Award Number: EXC 1069; Fundação para a Ciência e a Tecnologia, Grant/Award Number: PD/BD/114315/2016; German Academic Exchange Service, Grant/Award Number: 57340264; Open access funding enabled and organized by Projekt DEAL.

Abstract

Partition coefficients (K) of vitamins (riboflavin, nicotinic acid, nicotinamide, folic acid, cyanocobalamin) in aqueous two-phase systems (ATPS) composed by polyethylene glycol (PEG 4000, PEG 6000) and organic salt (sodium citrate and sodium tartrate) at T = 298.15 K and p = 1 bar have been studied. Data on liquid–liquid equilibria of the ATPS considered in this study have been taken from the literature (PEG-Na_3Citrate) or measured in this work (PEG-Na_2Tartrate) for PEG 4000 and PEG 6000 at T = 298.15 K and p = 1 bar. The experimental K values were validated by electrolyte perturbed-chain-statistical associating fluid theory predictions. The neutral cyanocobalamin has the highest K values among all studied vitamins at any ATPS studied in this work. This finding contrasted with expectations based on literature data which let assume that charged species have typically the highest K values in the considered ATPS. Thus, besides the typically strong charge–charge interactions especially specific forces (e.g., hydrogen bonding) explains the strong PEG-cyanocobalamin interaction resulting in the high K values.

KEYWORDS

citrate, partition coefficient, PEG, tartrate, weak electrolytes

1 | INTRODUCTION

Aqueous two-phase systems (ATPS) provide mild conditions for the partitioning of thermosensitive and water-prone organic molecules.[1-4] However, at least several of the commonly used phase formers within an ATPS may cause some environmental distress if applied at industrial scale.[5] A better alternative are biodegradable ATPS composed of nontoxic components, such as polyethylene glycol (PEG) and organic salts, for example, citrates or tartrates.[6-8] These environmentally friendly ATPS have been already considered for the separation of biomolecules such as antibiotics, DNP-amino acids, among others.[9-13] Presence of organic salt and high content of water in such ATPS are advantageous. However, due to many dependencies of the partitioning behavior, understanding the phenomena which rule the partitioning in these complex systems requires much more effort (e.g., data) than in conventional separation systems.[14,15] Solute partitioning in PEG–salt

[Correction added on Aug 24, 2020 after first online publication]

ATPS is highly influenced by pH, and both the pH and interactions strongly depend on the kind and composition (the tie-line length, *TLL*) of ATPS, as well as on the properties of ATPS phase formers, for example, PEG's molecular weight, type of anion, and cation of salt.[16]

The suitability of ATPS to separate different components can be evaluated experimentally based on partition coefficient (*K*) measurements. Prior to this, the binodal curves and phase compositions (tie-lines) of ATPS at equilibrium (*TLL*) must be determined. The binodal data allow a primary estimation of the potential cost of forming ATPS, as it gives information about the immiscibility region in phase diagrams. Although these data may be good enough to get some preliminary information on partitioning efficiency, *K* measurements over different *TLL* are decisive for choosing a system applicable to the separation of target components. By this, it becomes possible to evaluate the thermodynamic efficiency of an ATPS toward separation; the advantages of analyzing *K* values over *TLL* are (a) there is one parameter to describe the influence of ATPS composition on *K*, (b) it is possible to compare *K* of different solutes in the same ATPS and *TLL*, and (c) it is feasible to compare *K* of the same solute in different ATPSs but same *TLL*. Some previous studies show that *K* strongly depends on *TLL* of the ATPS and can either increase or decrease with increasing *TLL*.[11,17-19] For systems that show increased *K* values with increasing *TLL*, ATPS compositions are favored with high concentrations of the phase formers. This is rather undesired from environmental perspective and calls to search for different ATPSs that are more suitable for the partitioning of a given compound. This requirement is met by choosing biodegradable ATPS and this way it can overcome one of the biggest bottlenecks of ATPS claimed in the literature.[5]

Water-soluble vitamins have many applications and they were willingly applied among others as model drugs/ligands in controlled-release and targeting drug-delivery studies.[20-22] Being low water-soluble and ionizable components, many vitamins face similar problems compared to active pharmaceutical ingredients,[23] for example, low solubility, partial dissociation in aqueous systems. Additionally, water-soluble vitamins are appropriate model compounds to prove the ability of separation by ATPS caused by the high diversity of the molecular structures and properties of these vitamins. Consequently, vitamins might be then used as model-compounds for further partitioning of alike components in these ATPS. To the best of our knowledge, there has not been any work yet in which experimental data on partitioning of water-soluble vitamins in PEG–salt ATPS was reported.

The experimental effort can be much reduced with thermodynamic models that are capable to predict the partitioning of different vitamins in ATPS. In previous works, authors tried to describe and correlate partitioning of different compounds in ATPS using models for example, extended Chen-NRTL,[24] Wilson[25] in PEG–inorganic salt ATPS and with Pitzer model,[26] extended NRTL[27] and modified UNIQUAC[27] in PEG–organic salt ATPS. Also, one model based on Statistical Associating Fluid Theory (SAFT) has been used for the modeling of protein partitioning in PEG–inorganic salt ATPS.[28] However, predictions of the partitioning of organic solutes in PEG–organic salt ATPS using any predictive model have not been yet reported in literature. Perturbed-Chain SAFT (PC-SAFT) has been already proposed for modeling of vitamin partitioning just in conventional systems containing organic solvents and water.[29] To predict the partitioning of ionizable molecules in PEG–organic salt ATPS, it is of importance to consider the interactions of different ionic species in an electrolyte solution. This was done in the present work using electrolyte PC-SAFT (ePC-SAFT) model with an implemented Debye–Hückel term. ePC-SAFT has already been applied to predict the activity coefficients in weak electrolyte systems.[30] It has been also applied for predicting the liquid–liquid equilibria (LLE) of PEG–organic salt systems.[31] The conventional modeling approach used in the present work considers a homosegmented PEG chain. The required pure-component ePC-SAFT parameters were taken from the literature (PEG, Na^+, $Citrate^{3-}$, vitamins) or were estimated by fitting them to experimental densities and osmotic coefficients of binary water–Na_2Tartrate systems ($Tartrate^{2-}$).[32-38] The binary interaction parameters between phase formers (PEG, salt ions) were fitted to experimental tie-lines from the literature (PEG–Na_3Citrate) or to data determined in this work (PEG–Na_2Tartrate).[17] The partition coefficients of vitamins (VB2, $VB3^{acid}$, $VB3^{amide}$, VB9, VB12) were predicted using the activity coefficients obtained with ePC-SAFT in each phase and at different tie-line compositions.

The predictions were validated by new experimental partition-coefficient data. In this work *K* values were measured for five vitamins (riboflavin–VB2, nicotinic acid–$VB3^{acid}$, nicotinamide–$VB3^{amide}$, folic acid–VB9, and cyanocobalamin–VB12) in ATPS formed by PEG (PEG 4000, PEG 6000) and organic salt (Na_3Citrate, Na_2Tartrate) at T = 298.15 K and p = 1 bar. The binodal curves and equilibrium compositions were taken from the literature (PEG–Na_3Citrate) or measured in this study (PEG–Na_2Tartrate). The predictions were found to be in very good agreement to experimental data.

2 | BACKGROUND

2.1 | Dissociation equilibria of vitamins

At the pH of ATPS studied in this work (PEG–Na_3Citrate: pH 8.25 [bottom], 8.45 [top], PEG–Na_2Tartrate: pH 7.75 [bottom], 7.70 [top]) the water-soluble vitamins under consideration are negatively charged ($VB2^-$, $VB3^{acid-}$, $VB9^{2-}$, $VB9^{3-}$) or neutral ($VB3^{amide}$, VB12). The p*Ka* values necessary for the calculation of vitamin species distributions in each ATPS phase have been used as reported in the literature[39-47] (Table 1). The mean charge number q_{mean} of all vitamin species present in aqueous solution over different pHs is shown in Figure 1.

The behavior of vitamins in ATPS cannot be described without considering the equilibria expressions for ionizable compounds.[48] A detailed

TABLE 1 Dissociation constants (p*Ka*) for water-soluble vitamins at T = 298.15 K

Vitamin	pKa_1	pKa_2	pKa_3	pKa_4	Ref
VB2	1.7	6.1	10.2		39-43
$VB3^{acid}$	2.07	4.81			44
$VB3^{amide}$	3.35				45
VB9	2.38	3.34	4.7	8.1	46,47
VB12	1.82	13.99			43

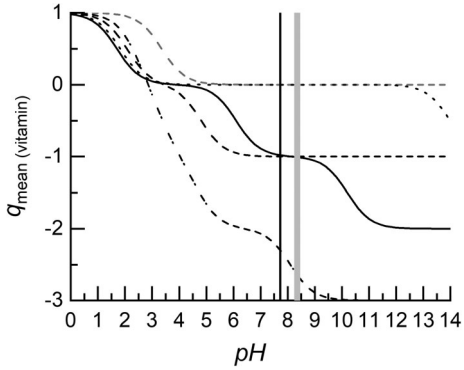

FIGURE 1 The mean charge number q_{mean} of all species in aqueous solution (calculated from the ionic distribution using p*K*a values from Table 1) as a function of pH. Lines: dashed—VB3 (gray—VB3^{amide}, black—VB3^{acid}), solid—VB2, dashed-dot—VB9, dotted—VB12. Vertical lines: PEG + Na_3Citrate (gray), PEG + Na_2Tartrate (black). The width of the vertical presents the pH range of the two phases of the aqueous two-phase systems (ATPSs)

description is included in Supplementary Information SI (Chapter S1, Table S1). To study the partitioning of vitamins considered in this work, it is necessary to look at the pH difference between the top and bottom phases of ATPS. Thus, the mole fractions of vitamin species were calculated for each phase of ATPS separately (SI Equations (S15) and (S16)).

2.2 | ePC-SAFT modeling

ePC-SAFT—which is based on original PC-SAFT—has been used in this work to model the ATPS containing ionizable components.[49] In ePC-SAFT, the residual Helmholtz energy ($a^{residual}$) is calculated with different energy contributions. The perturbations of the reference hard-chain system, which is represented by hard-chain forces ($a^{hard\ chain}$), origin from dispersive van der Waals attractions ($a^{dispersion}$), hydrogen bonding ($a^{association}$), and ionic interactions (a^{ion}).[50,51]

$$a^{residual} = a^{hard\ chain} + a^{dispersion} + a^{association} + a^{ion} \quad (1)$$

A component *i* is described by three pure-component parameters: the segment number (m_i^{seg}), the segment diameter (σ_i), and the dispersion-energy parameter (u_i/k_B). If this component is associating, two additional fitting parameters are introduced: the association-energy parameter ($\varepsilon^{A_iB_i}/k_B$), and the association-volume parameter ($k^{A_iB_i}$). Besides that, also the number of association sites (N_i^{assoc}) is assigned before modeling. As vitamins are ionizable components and they can be charged in the aqueous systems, the Coulomb interactions are considered by accounting for the charge. To model the mixtures with ePC-SAFT, combining rules from Berthelot–Lorentz[52,53] and Wolbach–Sandler[54] (Equations (2)–(5)) were used. Typically, the binary interaction parameter (k_{ij}) is required to model mixtures according to:

$$\sigma_{ij} = \frac{1}{2}\cdot\left(\sigma_i + \sigma_j\right) \quad (2)$$

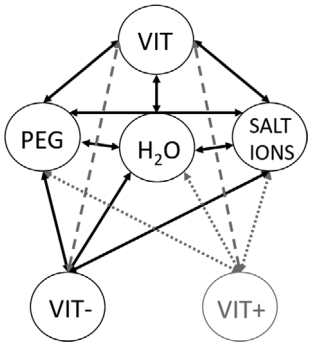

FIGURE 2 Interactions between components present in vitamin partitioning in the aqueous two-phase system (ATPS) considered in this work. Fractions of vitamin and salt depend on pH. Solid lines: the interactions considered in this work for electrolyte perturbed-chain (ePC)-statistical associating fluid theory (SAFT) modeling; dashed lines: theoretically possible interactions between different vitamins species present in aqueous solution—for simplification not considered in ePC-SAFT modeling; dotted lines: interactions which could be considered by ePC-SAFT if positively charged species were present in solution

$$u_{ij} = \sqrt{u_i \cdot u_j}\cdot\left(1 - k_{ij}\right) \quad (3)$$

$$\varepsilon^{A_iB_i} = \frac{1}{2}\cdot\left(\varepsilon^{A_iB_i} + \varepsilon^{A_jB_i}\right) \quad (4)$$

$$\kappa^{A_iB_i} = \sqrt{\kappa^{A_iB_i}\cdot\kappa^{A_iB_i}}\cdot\left(\frac{2\cdot\sqrt{\sigma_i\cdot\sigma_j}}{\left(\sigma_i+\sigma_j\right)}\right)^3 \quad (5)$$

For modeling the partitioning of vitamins in ATPS the interactions were considered as schematically presented in Figure 2. At pH ≈ 8 (considered in this work) just neutral species (VIT) and negatively charged (VIT^-) vitamin species are expected while the positive (VIT^+) species will not be present.

The activity coefficient of a component *i* was calculated using ePC-SAFT according to Equation (6), in which the fugacity coefficient of the mixture (φ_i) is divided by the fugacity coefficient of the pure component (φ_{0i}).

$$\gamma_i = \frac{\varphi_i}{\varphi_{0i}} \quad (6)$$

Activity coefficients are required for modeling the ATPS and the *K* values, see the following chapters.

2.3 | Phase equilibria of ATPS

Binary PEG/ion interaction parameters (k_{ij}) required in Equation (3) were fitted to LLE. Any LLE with *n* components is calculated through the isoactivity expression. In Equation (7), γ_i^I and γ_i^{II} represent the activity coefficients obtained with ePC-SAFT and x_i^I and x_i^{II} are the equilibrium mole fractions of component *i* in the phases I and II, respectively. To calculate the activity coefficients in ATPS, ePC-SAFT requires the parameters of all components present in solution.

$$x_i^I \gamma_i^I = x_i^{II} \gamma_i^{II} \quad i = 1, \ldots, n \tag{7}$$

2.4 | Partitioning of vitamins in ATPS

The experimentally accessible property is the partition coefficient $K_{vit,total}^{exp}$, which denotes the ratio of the total vitamin mole fraction in the first Phase *I* over the total vitamin mole fraction in the second Phase *II*. Access to modeling *K* values is realized by activity coefficients of the vitamin in the respective phases. As water-soluble vitamins are usually present at very small concentrations, the infinite dilution activity coefficient γ_{vit}^{∞} is very relevant, see Equation (8).

$$\lim_{x_{vit} \to 0} \gamma_{vit} = \gamma_{vit}^{\infty} \tag{8}$$

For neutral components, the procedure is rather simple. The case is different for charged vitamins. Depending on the pH of ATPS, several vitamins can be present as different species in solution. Thus, a connection between the experimentally observed $K_{vit,total}^{exp}$ and the value obtained by thermodynamic modeling is required. The partition coefficient at infinite dilution $K_{vit,j}^{pred,\infty}$ of a vitamin species *j* is defined as the concentrations ratio (in mole fraction and x_{vit}^I and x_{vit}^{II}) of species *j* in the two Phases *I* (PEG phase) and *II* (salt phase), respectively (Equation (9)).[55]

$$K_{vit,j}^{pred,\infty} = \frac{x_{vit,j}^I}{x_{vit,j}^{II}} = \frac{\gamma_{vit,j}^{\infty,II}}{\gamma_{vit,j}^{\infty,I}} \tag{9}$$

in which $\gamma_{vit}^{\infty,I}$ and $\gamma_{vit}^{\infty,II}$ are the activity coefficients at infinite dilution in the two phases. Partition coefficients higher than unity indicate that the vitamin species is partitioned mostly to the top (in this work: PEG) Phase *I*. If it is lower than one, the vitamin species are preferably present in the bottom (in this work: salt) Phase *II*.

The charge of vitamin species is explicitly considered in ePC-SAFT modeling. The ePC-SAFT pure-component parameters and binary interaction parameters for different species have been reported in the previous works.[29,35,38] The experimentally measured partition coefficient of a vitamin between the PEG phase and the salt phase is the total partition coefficient summed over all the vitamin species present in ATPS ($K_{vit,total}^{pred,\infty}$). This value differs from the ePC-SAFT predicted $K_{vit,j}^{pred,\infty}$ if $pH^I \neq pH^{II}$, where *I* and *II* are the Phases *I* and *II*. Conversion between the two values requires the species distributions (Equation (10)).

$$K_{vit,total}^{pred,\infty} = K_{vit,j}^{pred,\infty} \cdot \frac{\alpha_j^{II}}{\alpha_j^I} \tag{10}$$

Due to a difference in pH between the ATPS phases, the distributions of each vitamin species were calculated separately for Phases *I* and *II*. To determine the species fractions α_j^I and α_j^{II}, the p*K*a values from the previous Section 2.1 were used (SI, Equations (S15) and (S16)).

3 | MATERIALS AND EXPERIMENTAL METHODS

3.1 | Materials

The water-soluble vitamins considered in this work are riboflavin (VB2), nicotinic acid ($VB3^{acid}$), nicotinamide ($VB3^{amide}$), folic acid (VB9), and cyanocobalamin (VB12). PEG of two different average molecular weights: 4,000 and 6,000 g/mol has been purchased from Sigma-Aldrich. All the dilutions and stock solutions were prepared in deionized Millipore water (Merck KGaA). The vitamins stock solutions of VB3 were prepared just with water, while the stock solutions of poorly water-soluble VB2, VB9, and VB12, required adding sodium hydroxide dropwise to increase the solubility through pH change of 1 unit at maximum (final pH ≈ 6 for all three vitamin solutions). The CAS numbers, purities, and suppliers are provided in Table 2. All products were used as supplied without any further purification. The chemicals were weighted on Mettler Toledo analytical balance (XS205 Dual Range) with an uncertainty of ±0.01 mg.

3.2 | Measuring ATPS-phase diagrams

The binodal curves of the ATPS were determined with the cloud-point method according to the procedure previously reported in literature.[17,56] Different amounts of aqueous stock solutions, containing PEG and Na_2Tartrate, were added to assay tubes, thoroughly mixed in a vortex (VWR, model VV3) and placed in a thermostatic bath (Techne, Tempette TE-8D) at T = 298.15 ± 0.2 K. Then, water was added dropwise to the tubes using a syringe. The tubes were again mixed and located in a thermostatic bath. The procedure was repeated until one homogeneous phase was present. To determine the tie-lines, ATPS with different water + PEG + Na_2Tartrate feed compositions, within the biphasic region, were prepared in 15 ml tubes. The tubes were then vigorously shaken for 2 min in a vortex mixer and left for phase separation for at least 48 hr at T = 298.15 ± 0.2 K in a thermostatic bath. Preliminary studies pointed out these times as required for thorough mixing and total phase separation. Concentrations of PEG and salt were determined in both phases as described in literature.[17,56,57] Prior to this, the samples were withdrawn in triplicate with a syringe and appropriately diluted with water. The salt concentrations in each phase were measured in triplicate with a precision of ±0.5% at T = 298.15 K by electrical conductivity (Crison GLP31 Meter). The calibration curve was prepared using standard solutions of known salt concentration of 0.5–20 mM. In this range, no polymer interference was observed. Polymer concentrations in both phases were determined gravimetrically, after lyophilization according to published elsewhere procedure.[17,56,57] Samples of the top/bottom phase were diluted with water and frozen (T = 255 ± 1 K) for at least 24 hr. Then, they were placed in freeze-dryer for at least 72 hr. Following the procedure from the literature, the polymer concentrations were calculated by subtracting salt concentrations from masses of dried phase formers

TABLE 2 Sample provenance

Component[a]	CAS	Supplier	Mass fraction purity
VB2	83-88-5	Sigma	≥0.98
$VB3^{acid}$	59-67-6	Sigma-Aldrich	≥0.98
$VB3^{amide}$	98-92-0	Sigma-Aldrich	≥0.98
VB9	59-30-3	Sigma	≥0.97
VB12	68-19-9	Sigma	≥0.98
$Na_3Citrate$	6132-04-3	Sigma-Aldrich	≥0.99
$Na_2Tartrate$	6106-24-7	Sigma-Aldrich	≥0.99
PEG	25322-68-3	Sigma-Aldrich	
NaOH	1310-73-2	Sigma-Aldrich	≥0.97

[a]VB2 = riboflavin. $VB3^{acid}$ = nicotinic acid. $VB3^{amide}$ = nicotinamide. VB9 = folic acid. VB12 = cyanocobalamin. $Na_3Citrate$ = $Na_3C_6H_5O_7{\cdot}2H_2O$. $Na_2Tartrate$ = $Na_2C_4H_4O_6{\cdot}2H_2O$.

in each phase.[17,56,57] The *TLL* were determined as shown in Equation (11), where w_P^I, w_P^{II}, and w_S^I,w_S^{II} are the mass fractions of PEG or sodium salt in the top (I) and bottom (II) phases at equilibrium.

$$TLL = \sqrt{\left(w_P^I - w_P^{II}\right)^2 + \left(w_S^I - w_S^{II}\right)^2} \tag{11}$$

It is very common in literature to provide phase equilibrium compositions of ATPS in mass fractions and to calculate *TLL* based on this unit of concentration. Thus, for better data comparison between different sources, phase compositions are given in this work based on mass fraction. The mass fractions w_i can be converted to mole fractions x_i with Equations (12) and (13) (*P*–PEG, *S* [cation: Na^+, anion: $anion^-$]–salt, *W*–water). In these equations, v_i denotes the number of moles into which a salt dissociates in aqueous solution. In the ATPS studied in this work, citrates and tartrates fully dissociate leading to the presence of Na^+ and $Citrate^{3-}$ or $Tartrate^{2-}$ in a solution ($\alpha_{citrate^{3-}} = \alpha_{tartrate^{2-}} = 0.99$). For this reason, only these three ion species were considered for ePC-SAFT modeling.

$$x_i = \frac{\frac{w_i}{M_i}}{\frac{w_P}{M_P} + \left(v_{Na^+} + v_{anion^-}\right) \cdot \frac{w_S}{M_S} + \frac{w_W}{M_W}} \quad i = \text{PEG, water} \tag{12}$$

$$x_i = \frac{v_i \cdot \frac{w}{M_S}}{\frac{w_P}{M_P} + \left(v_{Na^+} + v_{anion^-}\right) \cdot \frac{w_S}{M_S} + \frac{w_W}{M_W}} \quad i = \text{Na+, anion} \tag{13}$$

Experimental results can be found in Figure S2, Table S2, and Table S3 (SI).

3.3 | Measuring partition coefficients

Measuring partitioning of vitamins in ATPS was carried out using the procedure previously published in literature.[11,17] ATPS were prepared from stock solutions containing PEG 4000 or PEG 6000 and salt ($Na_3Citrate$, $Na_2Tartrate$) according to Table S3 (SI). The additions of components were done using an automatic pipette (Multipipette XStream, Eppendorf). The tubes containing water, PEG and salt, with or without vitamin, were vigorously shaken for 2 min on a vortex mixer and right after that centrifuged for 15 min at 13.4×10^3 rpm (Minispin, Eppendorf) to obtain phase separation. For the next 2 hr, they were left at T = 298.15 K for total interface clearance. During this equilibration time, the temperature was controlled with air conditioning. Samples withdrawn in duplicate from each phase of ATPS (with or without vitamin) were appropriately diluted with water to avoid interferences from PEG and salt. Afterward, the absorbance of aliquots from the top and bottom phases were measured spectrophotometrically using ultraviolet–visible (UV–vis) spectroscopy at $\lambda_{max}(VB2)$ = 270 nm, $\lambda_{max}(VB3^{acid})$ = 260 nm, $\lambda_{max}(VB3^{amide})$ = 260 nm, $\lambda_{max}(VB9)$ = 280 nm, $\lambda_{max}(VB12)$ = 360 nm, and fluorescence $\lambda_{emission}(VB2)$ = 520 nm, $\lambda_{excitation}(VB2)$ = 270 nm (UV–VIS spectrophotometer: Thermo Scientific Varioskan Flash).[38] The absorbance was also determined for aliquots of ATPS not containing vitamin. These values were almost zero, ensuring that there are no interferences of PEG and salt in these measurements. From calibration curves (measured prior to this step), it was possible to calculate the mole fraction of vitamin in each phase for different tie-line compositions. The experimental partition coefficient $K_{vit,total}^{exp,x}$ at high vitamin dilution was determined using Equation (14).

$$K_{vit,total}^{exp,x} = \frac{x_{vit}^I}{x_{vit}^{II}} \tag{14}$$

Each vitamin considered in this work, except VB9, is fully present as just one species in both ATPS Phases *I* and *II*, and the total experimental partition coefficient $K_{vit,\ total}$ is then the same as for the respective species partition coefficient $K_{vit,\ j}$. In case of VB9, two species ($VB9^{2-}$, $VB9^{3-}$) will be present at the conditions under investigation (pH ≈ 8). Thus, both species will contribute to the total measured partition coefficient. The two species of VB9 ($VB9^{2-}$, $VB9^{3-}$) will be differently partitioned in ATPS due to a pH difference between the phases. This can be considered with Equation (15) which includes the species fractions α_j^I and α_j^{II} in Phases *I* (top) and *II* (bottom). These fractions are based on the pH-dependent species distribution in ATPS phases (results for species distribution can be found in SI in Table S1).

$$K_{vit,j}^{exp,x} = K_{vit,total}^{exp,x} \cdot \frac{\alpha_j^I}{\alpha_j^{II}} \quad (15)$$

Experimental results can be found in Tables S4 and S5 (SI).

4 | RESULTS AND DISCUSSION

4.1 | ePC-SAFT parameter estimation

The pure-component parameters and binary interaction ePC-SAFT parameters used in this work are presented in Tables 3 and 4, respectively. ePC-SAFT parameters for ATPS phase formers are available in the literature. Reschke et al.[31] presented a promising approach for ePC-SAFT modeling of ATPS containing organic salts and PEG with a lot of possible binary interaction parameters (copolymer approach for PEG and polysegmented approach for organic anion). In this work, we have compared the modeling approach from Reschke et al.[31] to the much simpler classical ePC-SAFT approach (homosegmented PEG, spherical Citrate^{3-}).[32-34] All parameters as well as the experimental ATPS data for this comparison were available in the literature for the LLE of the system water–PEG–Na_3Citrate at 298.15 K and 1 bar. The results are not shown here, but for the modeling of partitioning it was observed that both modeling strategies (Reschke[31] vs. classical ePC-SAFT with homosegmented PEG and spherical Citrate^{3-}) do not deviate much; please note, that the method of Reschke et al. has several other advantages, which is further discussed in Reschke.[31] However, in the following, the approach of Reschke[31] is not further used, and all results were obtained with classical ePC-SAFT revised from 2014. Please note, that the newest ePC-SAFT advancement of Bülow et al.[65] was not considered in this work as the parameters for all ions required in the present work are not yet available. The parameters for Tartrate^{2-} were fitted to experimental densities and osmotic coefficients of binary water–Na_2Tartrate solutions,[36,37] and Tartrate^{2-} was treated equally as

TABLE 3 ePC-SAFT pure-component parameters of all components considered in this work

Component	m_i^{seg} (–)	σ_i (Å)	u_i/k_B (K)	ε^{AiBi}/k_B (K)	κ^{AiBi} (–)	N_i^{assoc} [a]	Charge number (–)	Ref.
Water	1.205	[b]	353.95	2,425.67	0.045	1/1		58
VB2$^-$	15.924	2.63	150.315	2,548.11	0.034	5/5	–1	35
VB3^{acid-}	8.088	2.3522	209.045	1,088.56	0.002	3/1	–1	35, TW[c]
VB3^{amide}	4.649	1.7143	166.25	1,056.20	0.002	1/1	0	29
VB9^{2-}	16.717	2.6907	152.016	2,379.47	0.034	8/4	–2	35
VB9^{3-}	16.717	2.6907	152.016	2,379.47	0.034	10/2	–3	35
VB12	21.854	4.05	346.45	2,136.56	0.01	23/6	0	35,38
Na^+	1	2.82	230	—	—	—	+1	34
Citrate^{3-}	1	4.46	250	—	—	—	–3	32
Tartrate^{2-}	1	4.49	200	—	—	—	–2	TW[c]
PEG	M_{PEG}·0.050	2.9	204.6	1,799.80	0.02	2/2	0	33

Abbreviations: ePC-SAFT, electrolyte Perturbed-Chain Statistical Associating Fluid Theory.
[a]Association scheme: Acceptor/donor.
[b]σ_i = 2.7927 + 10.11·exp(–0.01775·T [K]) – 1.417·exp(–0.01146·T [K]).
[c]TW = this work.

TABLE 4 ePC-SAFT binary interaction parameters for all components considered in this work

	Na^+	Citrate^{3-}	Tartrate^{2-}	PEG	Water
Na^+	—	–1 [32]	–1	0	0.00046 [34]
Citrate^{3-}		—	—	0.1	–0.22687 [32]
Tartrate^{2-}		—	—	0.07	–0.2002
PEG				—	–0.135 [33]
VB2$^-$	0	0.39	0.29	0.142	-6.10×10^{-2} [35]
VB3^{acid-}	0	0.48	0.1	0	-6.30×10^{-2}
VB3^{amide}	0	0	–0.25	0	1.64×10^{-2} [29]
VB9^{2-}	0	0.92	0.6	0.159	-4.00×10^{-2} [35]
VB9^{3-}	0	0.95	0.45	0.11	-3.20×10^{-2} [35]
VB12	–0.2	–0.168	–0.08	0	-2.11×10^{-2} [35]

Abbreviations: ePC-SAFT, electrolyte Perturbed-Chain Statistical Associating Fluid Theory; PEG, polyethylene glycol.

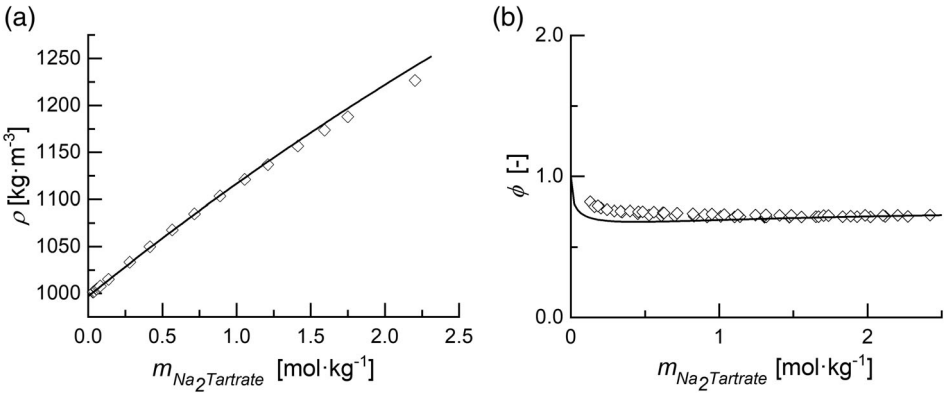

FIGURE 3 Densities ρ and osmotic coefficients ϕ of binary water–Na_2Tartrate system versus molality of Na_2Tartrate $m_{Na_2Tartarte}$ at T = 298.15 K, p = 1 bar. Experimental data (symbols) from literature.[36,37] Lines: electrolyte perturbed-chain (ePC)-statistical associating fluid theory (SAFT) modeling using parameters from Tables 3 and 4

TABLE 5 Modeling accuracies for all ATPS considered in this work (T = 298.15 K, p = 1 bar)

Salt	Polymer	*Np*	AAD (polymer phase)	AAD (salt phase)	AAD (both phase)
Na_3Citrate	PEG 4000	12	0.0303	0.00072	0.0155
Na_3Citrate	PEG 6000	12	0.0336	0.0246	0.0292
Na_2Tartrate	PEG 4000	12	0.0218	0.0323	0.0271
Na_2Tartrate	PEG 6000	12	0.0169	0.0359	0.0264

Abbreviations: AAD, average absolute deviation; ATPS, aqueous two-phase system; PEG, polyethylene glycol.

Citrate^{3-} as spherical ion. The results of this modeling are in good agreement with experimental data (Figure 3). The average relative deviation (ARD%) between ePC-SAFT modeling and experimental densities with *NP* number of data points was calculated with Equation (16) and yields ARD% = 0.38%. The deviations between experimental and modeled osmotic coefficients (ARD% = 3.46%) are also acceptable as experimental uncertainty is in the same order of magnitude.

$$ARD\% = 100 \cdot \frac{1}{NP} \cdot \sum_{k=1}^{NP} \left| 1 - \left(\frac{\rho^{mod}}{\rho^{exp}} \right)_k \right| \quad (16)$$

To accurately describe the interactions between the ATPS phase formers the binary PEG–salt ions interaction parameters (k_{ij}) were fitted to the equilibrium compositions from the literature or measured in this study.[17] Binodal data and tie-line data of ATPS are included in Tables S2 and S3 (SI), respectively. The tie-line concentrations of all components forming the ATPS were determined using isoactivity criteria with ion-averaged activities (more details are given elsewhere[34]). The average absolute deviations (AAD) calculated for both phases with Equation (17) were ≤0.029, which is an expected result for modeling ATPS compared to literature.[26,31]

$$\mathrm{AAD} = \frac{1}{l} \cdot \frac{1}{m} \cdot \frac{1}{n} \cdot \sum^{i} \sum_{i=1}^{m} \sum_{j=1}^{n} \left| w_i^{j,exp} - w_i^{j,mod} \right| \quad (17)$$

The AAD values from the modeling of all ATPS considered in this work are listed in Table 5. One example for modeling results of the ATPS PEG–Na_3Citrate for two different PEG molecular weights (4,000 and 6,000 g/mol) is presented in Figure 4, which illustrates the reasonable modeling results compared to experimental data. It is worth to note that these results only aimed at determining the interaction parameters between phase formers in ATPS as listed in Table 4. The ePC-SAFT modeled equilibrium compositions were not used as input for the prediction of the partition coefficients, rather the experimental equilibrium compositions were used for this purpose.

The pure-component parameters of vitamins were already published elsewhere.[29,35,38] The k_{ij} between water and negatively charged vitamins VB2$^-$, VB9^{2-}, and VB9^{3-} were fitted to pH-dependent solubility data in previous work.[38] The k_{ij} water–VB3^{acid-} was estimated in this study using pH-dependent solubilities reported in previous work and according to the approach from the literature (SI, Figure S1).[35] The k_{ij} values between vitamins and ATPS phase formers are considered with ePC-SAFT for the following pairs: vitamin–PEG, vitamin–Na^+, and vitamin–salt anion (Tartrate^{2-}, Citrate^{3-}). This modeling is described in more detail in the next sections.

4.2 | Predicting the vitamin partitioning in ATPS

Table S4 (SI) contains the mole-fraction based partition coefficients ($K^{exp,x}_{vit,total}$) of water-soluble vitamins VB2, VB3^{acid}, VB3^{amide}, VB9, and VB12 in ATPS composed by PEG (PEG 4000 or PEG 6000) and salt (Na_3Citrate or Na_2Tartarte). The partition behavior was studied at T = 298.15 K and p = 1 bar. ePC-SAFT pure-component parameters and the binary interaction parameters used for modeling are given in Tables 3 and 4. Overall, using these parameters enabled to predict the partition coefficients with reasonable accuracy. The ARD% between ePC-SAFT predictions and the experimental mole fraction-based K^x values are listed in Table 6.

While the pure-component parameters of vitamins and binary interaction parameters vitamin–water were taken from the literature,

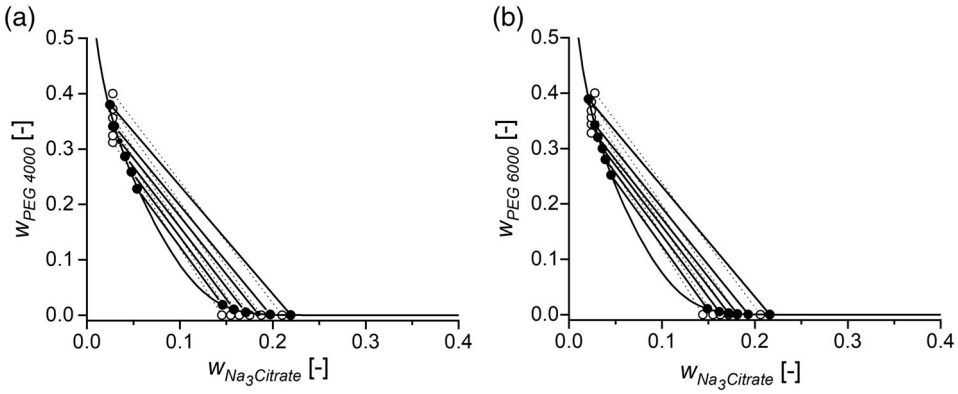

FIGURE 4 Aqueous two-phase system (ATPS) containing PEG (4,000–6,000) and $Na_3Citrate$ at T = 298.15 K, p = 1 bar: experimental[17] and ePC-SAFT (electrolyte Perturbed-Chain Statistical Associating Fluid Theory modeling). The equilibrium compositions are presented as circles: experimental (closed symbols) and ePC-SAFT modeling (open symbols). The solid lines (binodals, tie-lines)–experimental, dotted lines (tie-lines)–ePC-SAFT

TABLE 6 Prediction accuracies (expressed as ARD%) of partition coefficients of five water-soluble vitamins in each ATPS considered in this work (T = 298.15 K, p = 1 bar)

	ARD%			
Vitamin	**PEG 6000 + $Na_3Citrate$**	**PEG 4000 + $Na_3Citrate$**	**PEG 6000 + $Na_2Tartrate$**	**PEG 4000 + $Na_2Tartrate$**
$VB3^{amide}$	5.92	2.44	9.89	5.16
VB12	5.94	16.01	4.79	21.61
$VB3^{acid-}$	2.77	1.84	4.40	7.38
$VB2^{-}$	2.82	4.38	5.66	22.79
$VB9^{2-}$	3.48	7.15	4.41	10.89
$VB9^{3-}$	4.80	9.96	8.60	9.33

Abbreviations: ATPS, aqueous two-phase system; PEG, polyethylene glycol.

the binary interaction parameters vitamin–salt ions and vitamin–PEG were estimated in this work. The following procedure has been applied for the estimation of k_{ij}.

- *Negatively charged vitamins*: One rather very positive k_{ij} was required between each pair vitamin–anion (independent of M_{PEG}), and a slightly positive k_{ij} was applied to a pair vitamin–PEG (independent of M_{PEG}). Obviously, strong repulsion occurs between charged vitamin and the salt ions (especially the organic anions).
- *Neutral vitamins*: One k_{ij} was required between each pair vitamin–ion, and no parameter was required for vitamin–PEG. For $VB3^{amide}$ just one binary interaction parameter was introduced (vitamin–$Tartrate^{2-}$). This means that solely with parameters available in literature it was possible to predict K of $VB3^{amide}$ in ATPS composed by PEG (PEG 4000 or PEG 6000) and $Na_3Citrate$ with deviations ARD% ≤ 5.92. This is a very good result in a sense that ePC-SAFT could quantitatively predict K of $VB3^{amide}$ without introducing any additional binary parameters.

The number of ePC-SAFT binary interaction parameters (≤4) between species and ATPS phase formers used for the prediction of K is lower than the number of parameters used only for data correlation, for example, with extended Chen-NRTL (6 interaction parameters).[24] Also, the high deviations of extended Chen-NRTL of ≈30% between the experimental and correlated data have been much reduced with ePC-SAFT (Table 6). This is a great result; it means that using these parameters ePC-SAFT allows a priori predicting K values in similar systems with reasonable accuracy (Table 6).

The K values of water-soluble vitamins in ATPS composed by PEG and either one of two salts: $Na_3Citrate$ and $Na_2Tartrate$ is illustrated in Figure 5a,b. K values which are shown in Figure 5a,b can be influenced by many factors affecting the separation in ATPS. The effects on K of vitamins considered in the following Sections 4.2.1 and 4.2.2, respectively, are related to (a) vitamin interactions originating from a charge at pH of ATPS and molecular size of vitamin, or (b) interactions of vitamin with phase formers: the influence of TLL, salt type, PEG molecular weight.

4.2.1 | Influence of vitamin properties on vitamin partition coefficients in ATPS

The pH of ATPS can change the charge of vitamin.[59] As described in Section 2.1, the water-soluble vitamins are negatively charged ($VB2^{-}$, $VB3^{acid-}$, $VB9^{2-}$, $VB9^{3-}$) or neutral ($VB3^{amide}$, VB12) in the ATPS considered in this work (pH ≈ 8). At these conditions, VB2

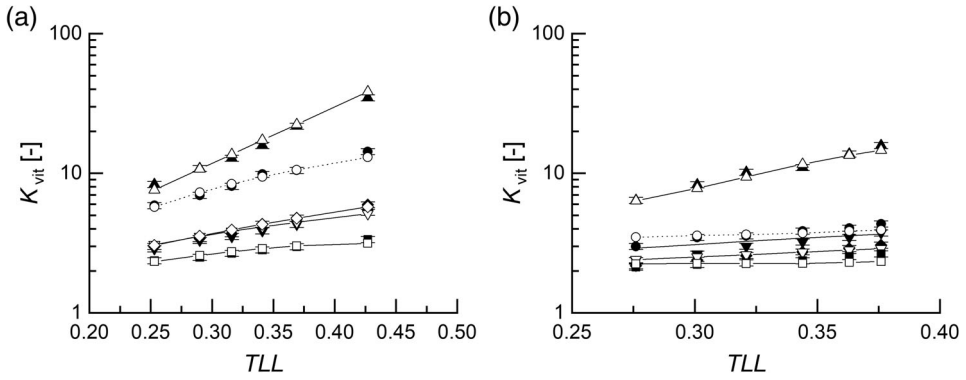

FIGURE 5 Partition coefficients at T = 298.15 K and p = 1 bar in aqueous two-phase system (ATPS): (a) PEG 6000–Na_3Citrate, (b) PEG 6000–Na_2Tartrate at different TL compositions. Experimental data $K^{exp,x}_{vit,total}$ measured in this work: closed symbols (Table S4, SI), ePC-SAFT (electrolyte Perturbed-Chain Statistical Associating Fluid Theory) predictions: open symbols. Vitamins: VB2 (circles), $VB3^{acid}$ (squares), $VB3^{amide}$ (up-to-down triangles), VB9 (diamonds), VB12 (triangles). Solid lines: the best fit to ePC-SAFT predictions of $K^{pred,\infty}_{vit,j}$—only to guide the eye, dotted lines: $K^{pred,\infty}_{vit,total}$ calculated using Equation (10) and ePC-SAFT predictions of $K^{pred,\infty}_{vit,j}$. Logarithmic scale was introduced for better data comparison

and $VB3^{acid}$ exist solely as single-negatively charged (−1) species $VB2^-$ and $VB3^{acid-}$. Others, $VB3^{amide}$ and VB12 are present exclusively as neutral species. In contrast, VB9 can be present as the two species, $VB9^{2-}$ and $VB9^{3-}$. These species are differently distributed between the phases. According to literature, more negatively charged molecules tend to partition into the more basic phase (in this case: PEG Phase *I*).[60] It is then expected that $VB9^{3-}$ will have higher K than $VB9^{2-}$ in ATPS considered in the present study. Equation (15) allows calculating the theoretical $K^{exp,x}_{vit,j}$ of each VB9 species j in ATPS by accounting on species distribution of VB9 at a given pH. The $K^{exp,x}_{vit,j}$ of species j = $VB9^{2-}$, $VB9^{3-}$, and the experimental value $K^{exp,x}_{vit,total}$ of VB9 in ATPS composed by PEG 6000 and Na_3Citrate are presented in Figure 6. The pure-component parameters needed to predict the partitioning of VB9 species in all ATPS from this study are given in Tables 3 and 4. The k_{ij} values for water–VB9 species were fitted in the previous study[35] to pH-dependent solubilities of VB9. The binary interaction parameters between one VB9 species and phase-forming components were fitted to one data point $K^{exp,x}_{vit,j}$ for each species. One data point means one tie-line in the ATPS composed by PEG 6000 and salt (Na_3Citrate or Na_2Tartrate). This procedure was accurate enough to predict partition coefficients very well over a wide range of *TLL*. $K^{pred,\infty}_{vit,total}$ were obtained using Equation (10). Besides that, the expected behavior as reported in the literature is observed: the most negative $VB9^{3-}$ possesses the highest K values,[60] which is reflected by to the very weak attractive interactions (very big k_{ij} values) between the multivalent negative VB9 species and the organic anions (see Table 4). The ARD% values presented in Table 6 prove that ePC-SAFT can very accurately predict the partition coefficients of VB9 species in PEG 6000–Na_3Citrate (ARD% ≤ 4.8%). Reasonable predictions of ARD% values ≤11% are observed for VB9 partitioning in all other systems considered in this work.

The partition coefficients of vitamins do not only depend on charge (on their species distribution), and thus not only on electrostatic

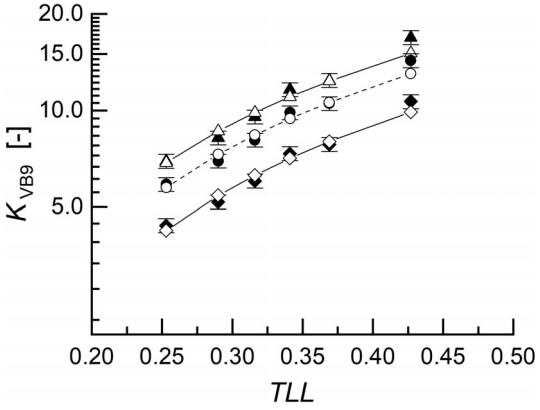

FIGURE 6 Partition coefficients of VB9 species K_{VB9} (circles), $K_{VB9^{2-}}$ (diamonds), $K_{VB9^{3-}}$ (triangles) in aqueous two-phase system (ATPS) PEG 6000–Na_3Citrate at different TL compositions, T = 298.15 K and p = 1 bar. Closed symbols: experimental data ($K^{exp,x}_{vit,total}$; total, contains $VB9^{2-}$ and $VB9^{3-}$) and data calculated with Equation (15) ($K^{exp,x}_{vit,j}$). Open symbols: ePC-SAFT (electrolyte Perturbed-Chain Statistical Associating Fluid Theory predictions) ($K^{pred,\infty}_{vit,j}$; species $VB9^{2-}$ or $VB9^{3-}$) and data calculated with Equation (10) ($K^{pred,\infty}_{vit,total}$). Lines are the best fit to ePC-SAFT predictions (solid lines— $K^{pred,\infty}_{vit,j}$ and dashed lines— $K^{pred,\infty}_{vit,total}$) applied only to guide the eye. Data measured in this work are presented in Table S4 (SI)

interactions. The strong pH-dependency of the partition coefficients shown in Figure 6 is caused by the presence of different VB9 species. However, the pH and thus electrostatic interactions are not dominating vitamin partitioning for those vitamins that are exclusively present at one species in the ATPS.[61] This can be seen in Figure 5, as the monovalent $VB3^{acid-}$ has just slightly higher K values than the neutral $VB3^{amide}$.

The partition coefficient can be influenced by steric entropic effects of the vitamins. VB3 is the smallest vitamin of lowest molecular weight over all studied in this work ($m_{VB3^{acid(-)}} = m_{VB3^{amide}}$ = 122.11 g/mol). The highest K determined in this work was found for VB12. This behavior can be explained by different effects related to the

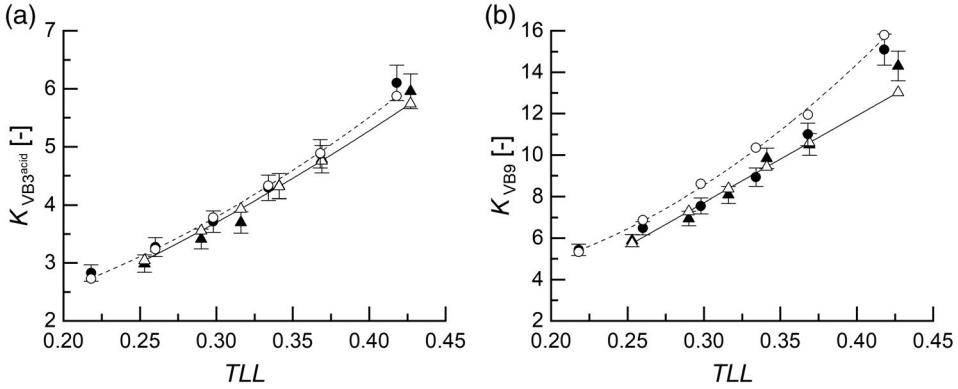

FIGURE 7 PEG molecular weight effect on partition coefficients of $VB3^{acid}$ and VB9 in aqueous two-phase system (ATPS) at T = 298.15 K and p = 1 bar. ATPS formed by PEG 4000 (dashed lines and circles)—Na_3Citrate and PEG 6000 (solid lines and triangles)—Na_3Citrate. Lines and open symbols: ePC-SAFT (electrolyte Perturbed-Chain Statistical Associating Fluid Theory) predictions (using parameters from Tables 3 and 4), closed symbols: experimental data. Lines represent the best fit to ePC-SAFT predictions applied only to guide the eye

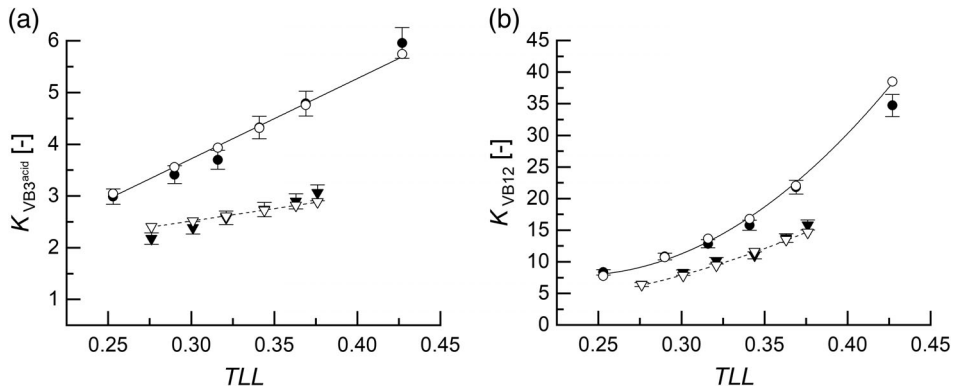

FIGURE 8 Anion effect on partition coefficients of $VB3^{acid}$ and VB12 in aqueous two-phase system (ATPS) at T = 298.15 K and p = 1 bar. ATPS formed by PEG 6000–Na_3Citrate (solid lines and circles) and PEG 6000–Na_2Tartrate (dashed lines and triangles). Lines and open symbols: ePC-SAFT (electrolyte Perturbed-Chain Statistical Associating Fluid Theory) predictions (using parameters from Tables 3 and 4), closed symbols: experimental data. Lines represent the best fit to ePC-SAFT predictions applied only to guide the eye

vitamin properties, for example, size-related effects. VB12 is neutral in PEG–Na_3Citrate and PEG–Na_3Tartrate ATPS; VB12 is structurally the most complex and the largest vitamin of all water-soluble vitamins (m_{VB12} = 1,355.37 g/mol). The high K values of VB12 might be caused by the fact that large molecules possess more possibilities (larger surface) of probable interactions with the ATPS phase formers.[60,62] These effects are often discussed in literature when the partitioning of large molecules, for example, proteins is studied.[3,61,62] It also confirms that the assumption used in literature when correlating K with Wilson model wrongly states that the partition can be explained solely in terms of charge effects.[25] Besides the fact that the very big VB12 just might have more interactions with PEG due to its size, it might additionally have also stronger interactions due to the presence of many diverse functional groups (hydrophobic interactions to PEG, or even hydrogen-bonding effects between PEG and VB12). All these enthalpic and entropic effects are considered explicitly in ePC-SAFT modeling.

4.2.2 | Influence of kind of ATPS phase formers on vitamin partition coefficients in ATPS

Changing PEG and salt concentrations influences the partitioning of vitamins in ATPS in a way that higher K are expected with increasing TLL (Figures 5–8). Increasing the salt concentration impacts the ionic strength, and the higher repulsion between salt anion and vitamin$^-$ might cause higher K values.[63,64] Altering PEG concentration might also influence K through favorable PEG–vitamin interactions[64] (e.g., increased cross-association). The higher K values are observed for citrate-based ATPS: ATPS composed by PEG and Na_2Tartrate (Figures 5 and 8) do allow only lower K values compared to ATPS formed by PEG and Na_3Citrate. This behavior might be related to the fact that the citrate-based salts cause higher repulsion to the vitamin species than the tartrate-based salts due to presence of higher valence of citrate (−3) over tartrate (−2). Besides, also PEG

molecular weight (4,000 or 6,000 g/mol) influences K values. K observed for ATPS formed by PEG 4000 are higher (Figure 7) than their pendants in ATPS formed by PEG 6000. Similar behavior has been already reported in the literature for other organic molecules, namely DNP-amino acids, partitioned in PEG 4000 or PEG 6000–Na_3Citrate ATPS.[17] The lower PEG molecular weight usually allows higher K values.[63] In general, it can be concluded that the highest K values are expected in a system formed by PEG with rather low molecular weight (preferably M_{PEG} < 4,000) and Na_3Citrate salt.

The influence of all system-dependent properties is also illustrated by the activity coefficients of the vitamin at infinite dilution in both phases, PEG phase and salt phase. The details are shown in the SI (Figures S3–S6). These diagrams show that the activity coefficients in the PEG phase are much lower than those in the salt phase. It might help other researchers to be able to relate the results on K values discussed in this manuscript to the activity coefficients that determine the modeled K values.

5 | CONCLUSIONS

Partitioning of organic compounds such as vitamins in PEG–organic salt ATPS strongly depends on the pH, as the vitamin might be present as different species depending on pH, and these species might have different partition coefficients. This is the reason why understanding the phenomena which rule the partitioning of vitamins in ATPS usually requires high experimental effort. In this work, the partition coefficients of five water-soluble vitamins over different tie-line compositions were determined experimentally. A modeling framework was developed within the thermodynamic model ePC-SAFT, which required pure-component and binary interaction parameters. Some of these parameters were already established and reported in the literature and were used in this work, while the binary interaction parameters between vitamin species and phase-forming components of the ATPS were estimated in the present study using only a very few experimental data points. In the modeling approach, the charge of the vitamins and the according species distribution depending on pH difference between the phases of ATPS were considered explicitly. The highest partition coefficient was observed for VB12, which might be related to large molecular size of VB12 and the strength of PEG-VB12 cross interactions. Further, the anion effect and PEG molecular weight influence on the vitamin partitioning were evaluated. The study shows that partitioning of vitamins in ATPS formed by citrate salt and PEG of lower molecular weight (PEG 4000) leads to the highest partition coefficients for all vitamins under consideration.

ACKNOWLEDGMENTS

Open access funding enabled and organized by Projekt DEAL.

ORCID

Kamila Wysoczanska https://orcid.org/0000-0001-7759-4802
Christoph Held https://orcid.org/0000-0001-8854-3234

REFERENCES

1. Mattiasson B. Applications of aqueous two-phase systems in biotechnology. *Trends Biotechnol*. 1983;1(1):16-20.
2. de Araujo Sampaio D, Mafra LI, Yamamoto CI, et al. Aqueous two-phase (polyethylene glycol+ sodium sulfate) system for caffeine extraction: equilibrium diagrams and partitioning study. *J Chem Thermodyn*. 2016;98:86-94.
3. da Silva NR, Ferreira LA, Madeira PP, Teixeira JA, Uversky VN, Zaslavsky BY. Analysis of partitioning of organic compounds and proteins in aqueous polyethylene glycol-sodium sulfate aqueous two-phase systems in terms of solute–solvent interactions. *J Chromatogr A*. 2015;1415:1-10.
4. Mittal R, Sharma R, Raghavarao K. Aqueous two-phase extraction of R-phycoerythrin from marine macro-algae, *Gelidium pusillum*. *Bioresour Technol*. 2019;280:277-286.
5. Espitia-Saloma E, Vâzquez-Villegas P, Rito-Palomares M, Aguilar O. An integrated practical implementation of continuous aqueous two-phase systems for the recovery of human IgG: from the microdevice to a multistage bench-scale mixer-settler device. *Biotechnol J*. 2016;11(5):708-716.
6. Tubío G, Pellegrini L, Nerli BB, Picó GA. Liquid–liquid equilibria of aqueous two-phase systems containing poly(ethylene glycols) of different molecular weight and sodium citrate. *J Chem Eng Data*. 2006;51(1):209-212.
7. Malpiedi LP, Fernández C, Picó G, Nerli B. Liquid–liquid equilibrium phase diagrams of polyethylene glycol+ sodium tartrate+ water two-phase systems. *J Chem Eng Data*. 2008;53(5):1175-1178.
8. Zafarani-Moattar MT, Hamidi A. Liquid–liquid equilibria of aqueous two-phase poly (ethylene glycol)–potassium citrate system. *J Chem Eng Data*. 2003;48(2):262-265.
9. Ghaffari S, Shahrouzi JR, Towfighi F, Khoshfetrat AB. Partitioning of cefazolin in aqueous two-phase systems containing poly (ethylene glycol) and sodium salts (citrate, tartrate, and sulphate). *Fluid Phase Equilibr*. 2019;488:54-61.
10. da Silva OS, Alves RO, Porto TS. PEG-sodium citrate aqueous two-phase systems to in situ recovery of protease from *Aspergillus tamarii* URM4634 by extractive fermentation. *Biocatal Agric Biotechnol*. 2018;16:209-216.
11. Wysoczanska K, Do HT, Held C, Sadowski G, Macedo EA. Effect of different organic salts on amino acids partition behaviour in PEG-salt ATPS. *Fluid Phase Equilibr*. 2018;456:84-91.
12. Afzal Shoushtari B, Rahbar Shahrouzi J, Pazuki G. Effect of nanoparticle additives on partitioning of cephalexin in aqueous two-phase systems containing poly (ethylene glycol) and organic salts. *J Chem Eng Data*. 2016;61(7):2605-2613.
13. Azevedo AM, Gomes AG, Rosa PA, Ferreira IF, Pisco AM, Aires-Barros MR. Partitioning of human antibodies in polyethylene glycol–sodium citrate aqueous two-phase systems. *Sep Purif Technol*. 2009;65(1):14-21.
14. Huddleston J, Veide A, Köhler K, Flanagan J, Enfors S-O, Lyddiatt A. The molecular basis of partitioning in aqueous two-phase systems. *Trends Biotechnol*. 1991;9(1):381-388.
15. Hatti-Kaul R. Aqueous two-phase systems. *Mol Biotechnol*. 2001;19(3):269-277.
16. Grilo AL, Raquel Aires-Barros M, Azevedo AM. Partitioning in aqueous two-phase systems: fundamentals, applications and trends. *Sep Purif Rev*. 2016;45(1):68-80.
17. Wysoczanska K, Macedo EA. Effect of molecular weight of polyethylene glycol on the partitioning of DNP-amino acids: PEG (4000, 6000) with sodium citrate at 298.15 K. *Fluid Phase Equilibr*. 2016;428:84-91.
18. Salabat A, Sadeghi R, Moghadam ST, Jamehbozorg B. Partitioning of L-methionine in aqueous two-phase systems containing poly (propylene glycol) and sodium phosphate salts. *J Chem Thermodyn*. 2011;43(10):1525-1529.

19. Dallora NLP, Klemz JGD, de Alcântara Pessôa Filho P. Partitioning of model proteins in aqueous two-phase systems containing polyethylene glycol and ammonium carbamate. *Biochem Eng J*. 2007;34(1):92-97.
20. Khosravian P, Shafiee Ardestani M, Khoobi M, et al. Mesoporous silica nanoparticles functionalized with folic acid/methionine for active targeted delivery of docetaxel. *Onco Targets Ther*. 2016;9:7315-7330.
21. Soppimath KS, Liu LH, Seow WY, et al. Multifunctional core/shell nanoparticles self-assembled from pH-induced thermosensitive polymers for targeted intracellular anticancer drug delivery. *Adv Funct Mater*. 2007;17(3):355-362.
22. Poschlad K, Enders S. Thermodynamics of aqueous solutions containing poly (N-isopropylacrylamide) and vitamin C. *Fluid Phase Equilibr*. 2011;302(1):153-160.
23. Avdeef A. Solubility of sparingly-soluble ionizable drugs. *Adv Drug Deliv Rev*. 2007;59(7):568-590.
24. Jimenez YP, Galleguillos HR, Claros M. Liquid-liquid partition of perchlorate ion in the aqueous two-phase system formed by NaNO3 + poly(ethylene glycol) + H2O. *Fluid Phase Equilibr*. 2016;421:93-103.
25. Madeira PP, Xu X, Teixeira JA, Macedo EA. Prediction of protein partition in polymer/salt aqueous two-phase systems using the modified Wilson model. *Biochem Eng J*. 2005;24(2):147-155.
26. Perez B, Malpiedi LP, Tubío G, Nerli B, de Alcântara Pessôa Filho P. Experimental determination and thermodynamic modeling of phase equilibrium and protein partitioning in aqueous two-phase systems containing biodegradable salts. *J Chem Thermodyn*. 2013;56:136-143.
27. Edrisi S, Bakhshi H, Rahimnejad M. Aqueous two-phase systems for cephalexin monohydrate partitioning using poly ethylene glycol and sodium tartrate dihydrate: experimental and thermodynamic modeling. *Korean J Chem Eng*. 2019;36(5):780-788.
28. Doozandeh SG, Pazuki G, Asghar A. Study of protein partitioning in polymer-salt aqueous two-phase systems using electrolyte-SAFT (E-SAFT) equation of state. *J Dispers Sci Technol*. 2012;33(5):756-762.
29. Laube F, Klein T, Sadowski G. Partition coefficients of pharmaceuticals as functions of temperature and pH. *Ind Eng Chem Res*. 2015;54(15):3968-3975.
30. Held C, Sadowski G. Modeling aqueous electrolyte solutions. Part 2. Weak electrolytes. *Fluid Phase Equilibr*. 2009;279(2):141-148.
31. Reschke T, Brandenbusch C, Sadowski G. Modeling aqueous two-phase systems: III. Polymers and organic salts as ATPS former. *Fluid Phase Equilibr*. 2015;387:178-189.
32. Wangler A, Loll R, Greinert T, Sadowski G, Held C. Predicting the high concentration co-solvent influence on the reaction equilibria of the ADH-catalyzed reduction of acetophenone. *J Chem Thermodyn*. 2019;128:275-282.
33. Stoychev I, Galy J, Fournel B, Lacroix-Desmazes P, Kleiner M, Sadowski G. Modeling the phase behavior of PEO−PPO−PEO surfactants in carbon dioxide using the PC-SAFT equation of state: application to dry decontamination of solid substrates. *J Chem Eng Data*. 2009;54(5):1551-1559.
34. Held C, Reschke T, Mohammad S, Luza A, Sadowski G. ePC-SAFT revised. *Chem Eng Res Des*. 2014;92(12):2884-2897.
35. Wysoczanska K, Macedo EA, Sadowski G, Held C. Solubility enhancement of water-soluble vitamins in the presence of covitamins: measurements and ePC-SAFT assisted predictions. *Ind Eng Chem Res*. 2019;58:21761-21771. https://doi.org/10.1021/acs.iecr.9b04302.
36. Zafarani-Moattar MT, Hosseinzadeh S. Refractive index, viscosity, density, and speed of sound of aqueous sodium tartrate solutions at various temperatures. *J Chem Eng Data*. 2006;51(4):1190-1193.
37. Zafarani-Moattar MT, Hamzehzadeh S, Hosseinzadeh S. Phase diagrams for liquid–liquid equilibrium of ternary poly(ethylene glycol) +di-sodium tartrate aqueous system and vapor–liquid equilibrium of constituting binary aqueous systems at T=(298.15, 308.15, and 318.15)K: experiment and correlation. *Fluid Phase Equilibr*. 2008;268(1):142-152.
38. Wysoczanska K, Sadowski G, Macedo EA, Held C. Toward thermodynamic predictions of aqueous vitamin solubility: an activity coefficient-based approach. *Ind Eng Chem Res*. 2019;58(17):7362-7369.
39. Rivlin R. *Riboflavin*. Plenum Press, New York: Springer Science & Business Media; 2012.
40. Kuhn R, Moruzzi G. Über das reduktions-oxydations-potential des lactoflavins und seiner derivate. *Ber Dtsch Chem Ges*. 1934;67(7):1220-1223.
41. Suelter CH. Mechanism of oxidation of reduced pyridine nucleotide analogs by riboflavin. 1959.
42. Michaelis L, Schubert MP, Smythe C. Potentiometric study of the flavins. *J Biol Chem*. 1936;116:587-607.
43. Calculation module developed by ChemAxon [computer program]: Calculation module developed by ChemAxon; 2019.
44. Klingsberg E. *Pyridine and its Derivatives*. Vol 32. Interscience Publishers, Inc., New York, Interscience Publishers, Inc., London: John Wiley & Sons; 2009.
45. Perrin DD. *Dissociation Constants of Organic Bases in Aqueous Solution: Supplement*. Butterworths: London; 1972.
46. Szakács Z, Noszál B. Determination of dissociation constants of folic acid, methotrexate, and other photolabile pteridines by pressure-assisted capillary electrophoresis. *Electrophoresis*. 2006;27(17):3399-3409.
47. Hofsäss MA, de Souza J, Silva-Barcellos NM, et al. Biowaiver monographs for immediate-release solid oral dosage forms: folic acid. *J Pharm Sci*. 2017;106(12):3421-3430.
48. Avdeef A. *Absorption and Drug Development: Solubility, Permeability, and Charge State*. New Jersey: John Wiley & Sons; 2012.
49. Gross J, Sadowski G. Perturbed-chain SAFT: an equation of state based on a perturbation theory for chain molecules. *Ind Eng Chem Res*. 2001;40(4):1244-1260.
50. Gross J, Sadowski G. Application of perturbation theory to a hard-chain reference fluid: an equation of state for square-well chains. *Fluid Phase Equilibr*. 2000;168(2):183-199.
51. Cameretti LF, Sadowski G, Mollerup JM. Modeling of aqueous electrolyte solutions with perturbed-chain statistical associated fluid theory. *Ind Eng Chem Res*. 2005;44(9):3355-3362.
52. Berthelot D. Sur le mélange des gaz. *Compt Rendus*. 1898;126:1703-1706.
53. Lorentz HA. Ueber die anwendung des satzes vom virial in der kinetischen theorie der gase. *Ann Phys*. 1881;248(1):127-136.
54. Wolbach JP, Sandler SI. Using molecular orbital calculations to describe the phase behavior of cross-associating mixtures. *Ind Eng Chem Res*. 1998;37(8):2917-2928.
55. Von Stockar U, van der Wielen LAM. *Biothermodynamics: The Role of Thermodynamics in Biochemical Engineering*, Lausanne, Switzerland: EPFL Press, 2013.
56. Silvério SC, Wegrzyn A, Lladosa E, Rodríguez O, Macedo EA. Effect of aqueous two-phase system constituents in different poly (ethylene glycol)–salt phase diagrams. *J Chem Eng Data*. 2012;57(4):1203-1208.
57. Silvério SC, Rodríguez O, Teixeira JA, Macedo EA. Liquid−liquid equilibria of UCON+(sodium or potassium) phosphate salt aqueous two-phase systems at 23 C. *J Chem Eng Data*. 2009;55(3):1285-1288.
58. Fuchs D, Fischer J, Tumakaka F, Sadowski G. Solubility of amino acids: influence of the pH value and the addition of alcoholic cosolvents on aqueous solubility. *Ind Eng Chem Res*. 2006;45(19):6578-6584.
59. Banik R, Santhiagu A, Kanari B, Sabarinath C, Upadhyay S. Technological aspects of extractive fermentation using aqueous two-phase systems. *World J Microbiol Biotechnol*. 2003;19(4):337-348.
60. Peters, T.J. (1987), *Partition of cell particles and macromolecules: Separation and purification of biomolecules, cell organelles, membranes and cells in aqueous polymer two phase systems and their use in biochemical analysis and biotechnology*. P-A. Albertsson. Third Edition, 1986, John Wiley and Sons, Chichester. Book review.

61. Andrews B, Schmidt A, Asenjo J. Correlation for the partition behavior of proteins in aqueous two-phase systems: effect of surface hydrophobicity and charge. *Biotechnol Bioeng*. 2005;90(3):380-390.
62. Walter H, Brooks DE, Fisher D. *Partitioning in Aqueous Two-Phase Systems*. Academic Press: NewYork; 1985.
63. Amid A. *Recombinant Enzymes—From Basic Science to Commercialization*. Springer: Springer, Cham; 2015.
64. Raja S, Murty VR, Thivaharan V, Rajasekar V, Ramesh V. Aqueous two phase systems for the recovery of biomolecules—a review. *Sci Technol*. 2011;1(1):7-16.
65. Bülow M, Ji X, Held C. Incorporating a concentration-dependent dielectric constant into ePC-SAFT. An application to binary mixtures containing ionic liquids. *Fluid Phase Equilibr*. 2019;492:26-33.

SUPPORTING INFORMATION

Additional supporting information may be found online in the Supporting Information section at the end of this article.

How to cite this article: Wysoczanska K, Do HT, Sadowski G, Macedo EA, Held C. Partitioning of water-soluble vitamins in biodegradable aqueous two-phase systems: Electrolyte perturbed-chain statistical associating fluid theory predictions and experimental validation. *AIChE J*. 2020;66:e16984. https://doi.org/10.1002/aic.16984